Supplementary

Figure S1. Hydrothermal features, and selected Mn ore styles and Mn mineralized microbially induced sedimentary structures (MISS), Cape Vani Mn oxide deposit. A. Stringer Mn deposits. Mn mineralised barite(±silica) veins stringer networks crosscut stratiform Mn ore, Mn nodules, bedded barite ore, and cross-bedded sandstone/sandy tuff host (Vani vein/Figure X). B. MISS type: Nodules. Loaf- to mound-shaped structures with nodular and cauliflower-like thrombolytic surface fabric (VA-05-16/Table S1). C. MISS type: Mat fragments and chips. Plan view of upper bedding surface of unmineralized sandstone/sandy tuff covered by large patches of millimeter-thick Mn crusts, with highly irregular outlines and embayments, crosscut by white smoker–type hydrothermal-exhalative barite (-silica) feeder veinlets (black arrows). Chisel is 21 cm long (SMO-05-10/Table S1). D. MISS type: Mat-Layer Structure. Upper bedding surface showing ''mat layer structure.'' Concentric rims with crenulated appearance and discoidal colony texture (dotted line) (VA-05-05/Table S1). E. MISS type: Upturned and Curled Margins. Cracks with upturned and curled margins on upper surface of fine-grained Mn sandstone/sandy tuff. Curved and upturned (involute) margin (arrow) of inferred fossil microbial mat consists of Mn-rich sandstone. Chisel in C is 21 cm (MI-04-27/Table S1). F. Mn sandstone/sandy tuff—chimney. Tubular cone possibly representing a white smoker structure, consisting of erratic and locally patchy amounts of Mn oxides and barite that cement epiclastic sandstone and sandy tuff; knolls of Mn oxide minerals are adhering to the outer surface and tip of cone [VA-05-06/Table S1]. Number of analysed sample/Table with mineralogical composition or Figure with EPR analysis.

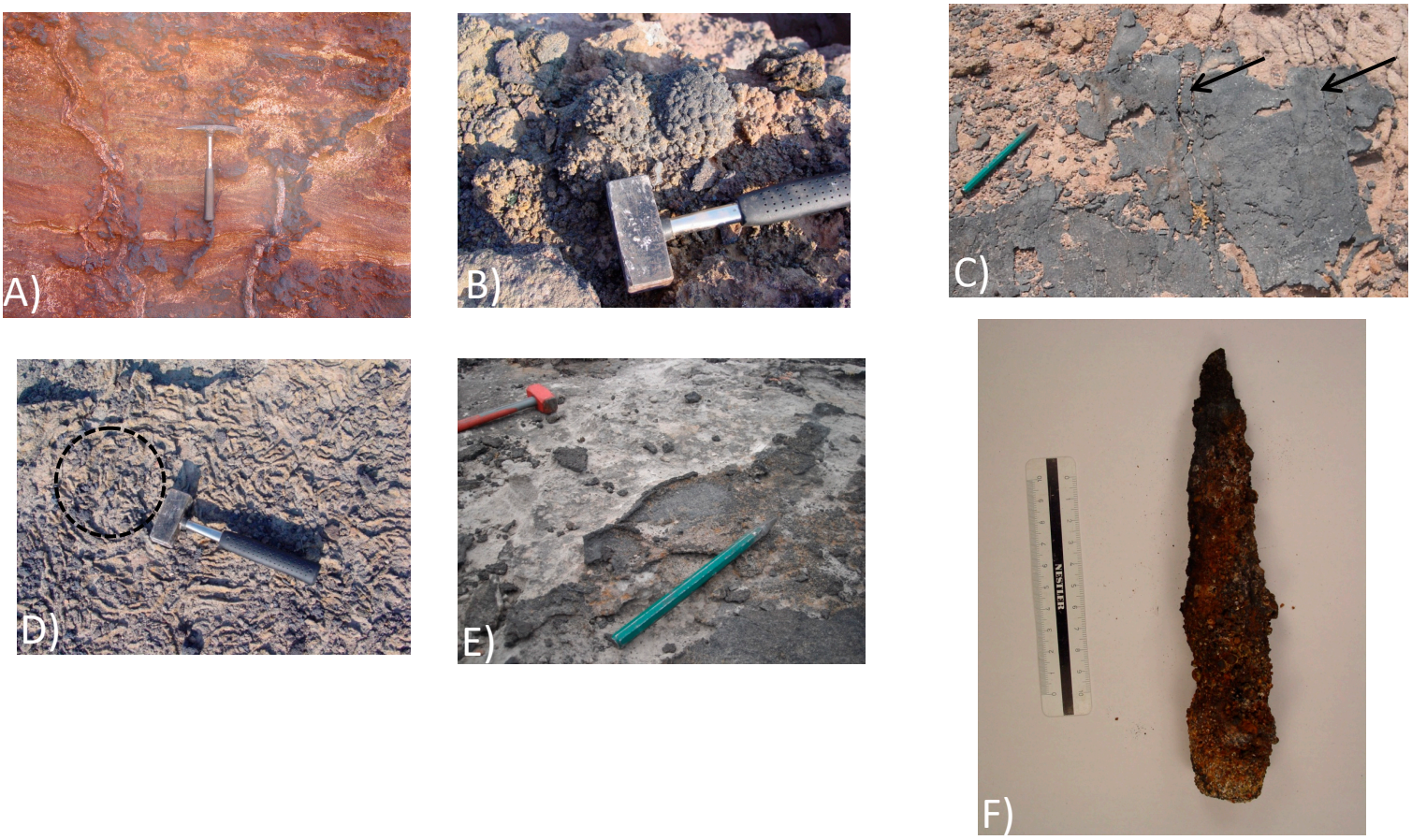

Figure S2. Representative X-ray powder diffraction pattern obtained for todorokite(T)-rich samples

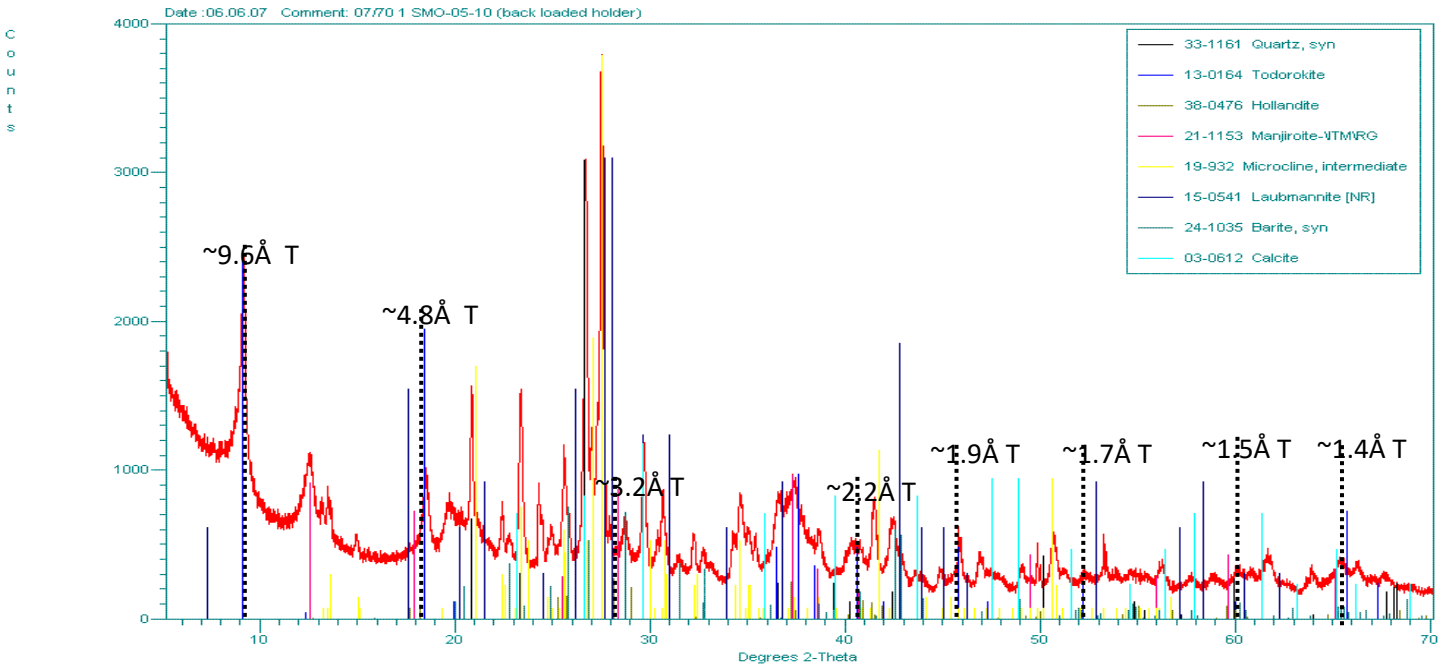

Figure S3. Representative X-ray powder diffraction patterns obtained for manjiroite (M)-rich samples [http://webmineral.com/data/Manjiroite.shtml#.VWSoEkbHd5V; [1]; http://rruff.info/Manjiroite]

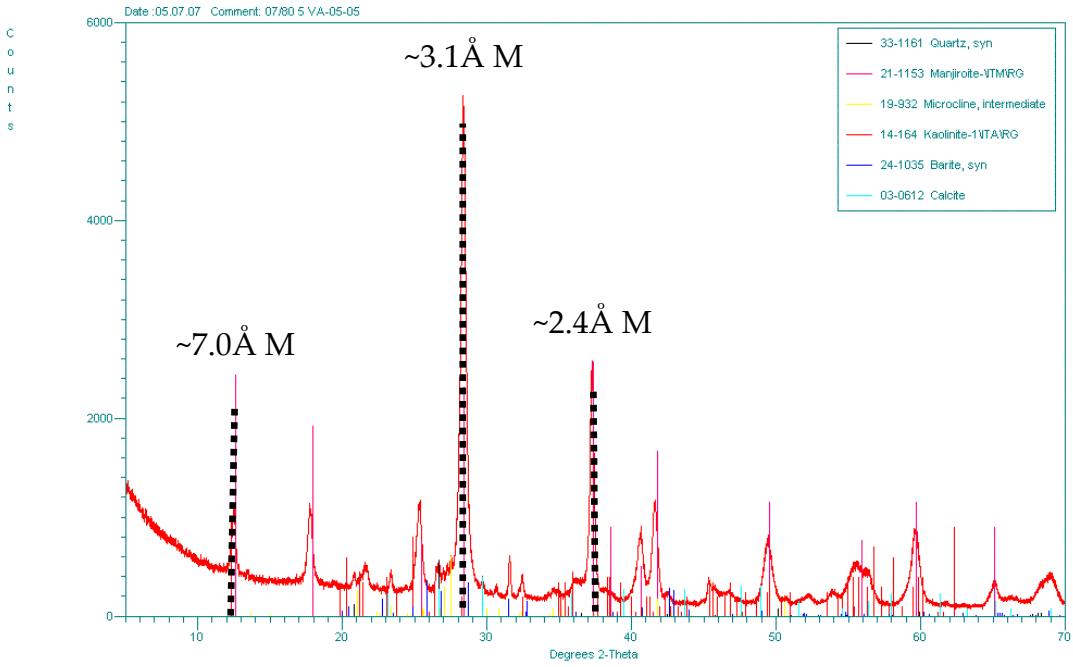

Figure S4. (a) SEM-backscattered electron (**BSE**) image of elongated fibres of crystalline todorokite (>5 µm) intergrown within a platy todorokite matrix which cement K-feldspar microclasts (K); (b) FEG-SEM image of nanocrystalline todorokite in the form of fibrous needles (<0.4 µm) intergrown within a platy Mn oxide matrix; these fibres appear to be aggregated into a dense network of fibres displaying a plate-like growth morphology which is characteristic of synthetic todorokite transformed from birnessite [2].

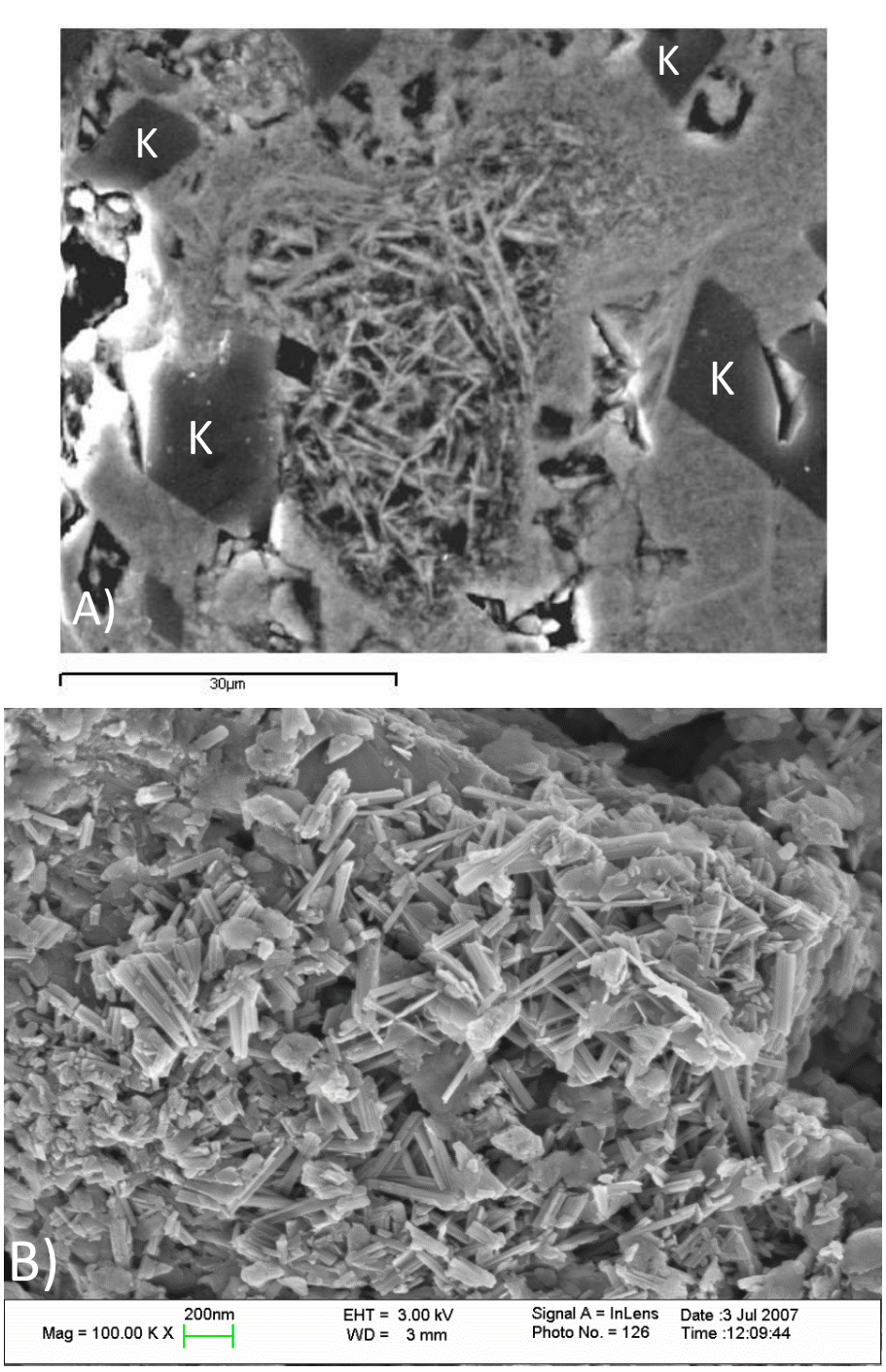

Figure S5. FEG-SEM EDS image and elemental maps of todorokite nanoplatelets. Image scale bar is 500 nm.

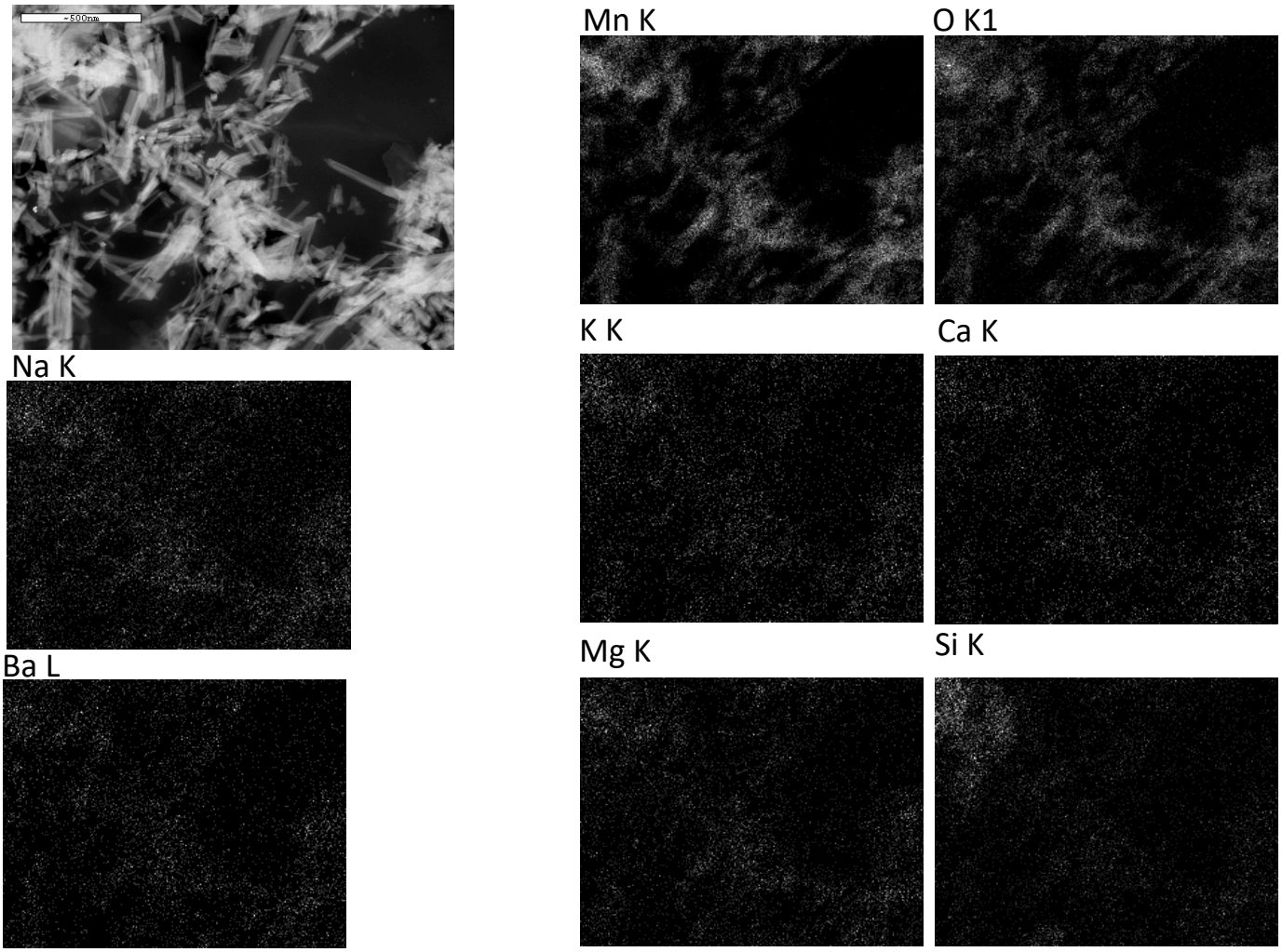

Sample	Mineralogy	Ore type/MnMISS type*
SMO-05-09	Hollandite, todorokite, manjiroite, K-feldspar, barite, quartz, illite	Stratiform Mn/growth bedding structures
SMO-05-05	Hollandite, K-feldspar, barite, quartz	Stratiform Mn/growth bedding structures
SMO-05-10	Todorokite, K-feldspar, hollandite, manjiroite, barite, laubmannite(?)	Mn sandstone/sandy tuff/mat fragments and chips
VA-05-05	Manjiroite, K-feldspar, barite, quartz, kaolinite	Mn crusts/mat-layer structure
VA-05-06	Todorokite, manjiroite, hollandite, K-feldspar, quartz, illite, kaolinite	Mn sandstone/sandy tuff/Chimney
VA-05-10	Todorokite, manjiroite, K-feldspar, quartz laubmannite(?)	Mn sandstone/sandy tuff/growth bedding structures
VA-05-16	Todorokite, hollandite, K-feldspar, quartz, barite, kaolinite	Mn crusts/Mn nodules
MI-04-27	Hollandite, todorokite, K-feldspar, manjiroite, quartz, barite	Mn crusts/upturned-curled margins
MI-04-36	Hollandite, todorokite, , K-feldspar, quartz, barite, kaolinite	Mn crusts/Fossil gas domes
clastic	Todorokite, K-feldspar, hollandite, manjiroite, barite, laubmannite(?)	Mn sandstone/sandy tuff/growth bedding structures and nodules

Table S1. Powder X-ray diffraction mineralogy of various Ore/MnMISS types

*Kilias (2012) [3]

Table S2. SEM-EDX spot analyses of crystalline todorokite (Figure S4B). Values in weight %.

Sample SMO-05-10	Na_2O	MgO	SiO_2	K_2O	CaO	MnO(MnO_2)	ZnO	Cl_2O	BaO	Al_2O_3
Analysis 1	3.1	3.33	0.26	0.88	0.82	67.68(82.84)			2.43	
Analysis 2	2.39	3.16		0.73	0.74	67.54(82.77)			2.49	
Analysis 7	1.56	1.77		0.73	0.56	64.60(79.16)	1.03		2.92	
Analysis 8	2.02	3.11		0.93	0.92	65.83(80.67)	0.94		2.73	
Analysis 9	2.77	2.73		0.83	0.75	65.70(80.51)		0.33	2.13	
Analysis 10	2.01	2.32	0.52	0.75	0.59	60.68(74.36)		0.29	2.79	0.5
Analysis 11	2.71	2.53	2.43	1.11	0.74	65.29(80.01)	0.94		2.26	1.16
Analysis 12	2.4	2.79	0.49	0.82	0.86	65.77(80.60)	1.3	0.35	2.88	0.66
Analysis 15	1.72	2.42	0.26	0.67	1.01	62.44(76.51)	1.0		2.48	0.57

References

1. Gutzmer, J.; Beukes, N.J. Asbestiform manjiroite and todorokite from the Kalahari manganese field, South Africa. *South African J. Geol.* **2000**, 103, 163-174.
2. Atkins, A.L.; Shaw, S.; Peacock, C.L. Nucleation and growth of todorokite from birnessite: Implications for trace-metal cycling in marine sediments. *Geochim. Cosmochim. Acta* **2014,** *144*, 109-125.
3. Kilias, S.P. Microbial Mat–Related Structures in the Quaternary Cape Vani Manganese-Oxide (-Barite) Deposit, NW Milos Island, Greece. In Microbial Mats in Siliciclastic Depositional Systems through Time; SEPM Special Publication: Athen, Greece, **2012**; Volume 101, pp. 97–110.